# Thermoelectric performance of electron and hole doped PtSb2

# Thermoelectric performance of electron and hole doped PtSb2

Y. Saeed, N. Singh, D. Parker, and U. Schwingenschlögl

Citation: Journal of Applied Physics **113**, 163706 (2013); doi: 10.1063/1.4803145
View online: http://dx.doi.org/10.1063/1.4803145
View Table of Contents: http://scitation.aip.org/content/aip/journal/jap/113/16?ver=pdfcov
Published by the AIP Publishing

# Thermoelectric performance of electron and hole doped $PtSb_2$

Y. Saeed,[1] N. Singh,[1] D. Parker,[2] and U. Schwingenschlögl[1,a)]
[1]*Physical Science & Engineering Division, KAUST, Thuwal 23955-6900, Kingdom of Saudi Arabia*
[2]*Materials Science and Technology Division, Oak Ridge National Laboratory, Oak Ridge, Tennessee 37831-6056, USA*

(Received 27 February 2013; accepted 12 April 2013; published online 30 April 2013)

We investigate the thermoelectric properties of electron and hole doped $PtSb_2$. Our results show that for doping of 0.04 holes per unit cell ($1.5 \times 10^{20}$ cm$^{-3}$) $PtSb_2$ shows a high Seebeck coefficient at room temperature, which can also be achieved at other temperatures by controlling the carrier concentration (both electron and hole). The electrical conductivity becomes temperature independent when the doping exceeds some 0.2 electrons/holes per unit cell. The figure of merit at 800 K in electron and hole doped $PtSb_2$ is comparatively low at 0.13 and 0.21, respectively, but may increase significantly with As alloying due to the likely opening of a band gap and reduction of the lattice thermal conductivity. © *2013 AIP Publishing LLC*. [http://dx.doi.org/10.1063/1.4803145]

## I. INTRODUCTION

Efficient thermoelectric materials are currently a striking challenge for researchers.[1] In general, the efficiency is determined by the figure of merit $ZT = \sigma S^2 T/\kappa$, where $\sigma$ is the electrical conductivity, $S$ is the Seebeck coefficient, $T$ is the temperature, and $\kappa$ is the thermal conductivity. To achieve a high $ZT$, $\sigma$ and $S$ should be large, while at the same time $\kappa$ should be small. However, increasing $\sigma$ by increasing the carrier concentration usually decreases $S$ and increases $\kappa$. Therefore, it is a prime task to control the numerator $\sigma S^2$ (the powerfactor) and the denominator $\kappa$ independently.

Kuroki and coworkers have shown that a metal with pudding mold type bands (a dispersive portion and a flat portion) can exhibit good thermoelectric properties.[2] Recently, such bands have been reported in the cubic pyrite material $PtSb_2$, which has a high $S = 250\,\mu$VK$^{-1}$.[3] Bulk $PtSb_2$ can be both metallic and semiconducting for deviations from the ideal stoichiometry, and it can be $n$- and $p$-type doped with charge carrier concentrations spanning several orders of magnitude ($10^{16}$ cm$^{-3}$ to $10^{20}$ cm$^{-3}$), as observed for different synthesis methods and parameters.[4–9] While $p$-doping (by Ir doping on the Pt site) gives a high metallic conductivity and large Seebeck coefficient,[3] $n$-doping (by Sb deficiency) gives a large Seebeck coefficient and thermal conductivity between 0 and 300 K.[10] $PtSb_2$ has a high mobility due to a small difference in the electronegativities of Pt and Sb (2.28 and 2.05, respectively).[11]

In the present work, we address the effect of electron and hole doping in $PtSb_2$, which has a melting temperature of 1500 K,[12] on $\sigma$ and $S$ from 300 K to 800 K. We study the powerfactor and the figure of merit for both types of doping. We also address the thermopower of $PtAs_2$ and the likely effects of alloying $PtSb_2$ with As.

## II. COMPUTATIONAL METHOD AND RESULTS

We calculate the band structure of $PtSb_2$ using density function theory as implemented in the WIEN2K package.[13] The popular generalized gradient approximation[14] is employed to optimize the volume and the internal atomic coordinates. To simulate doping, we use the virtual crystal approximation[15] and rigid band approach.[16,17] This approximation is widely employed in calculations of transport properties of doped semiconductors and is accurate when the doping is not too large. After having reached self-consistency in the calculations, we employ the post-processing BoltzTraP code[18] to calculate the thermopower. This tool has demonstrated quantitative accuracy in calculating the thermopower of metals and doped semiconductors.[19–22] We use 3000 **k**-points in the full Brillouin zone for calculating the electronic structure and a dense mesh of 3564 **k**-points in the irreducible wedge of the Brillouin zone for the thermoelectric calculations. $PtSb_2$ crystallizes in a cubic pyrite structure with space group $Pa\bar{3}$ and, therefore, exhibits isotropic transport properties. Our optimized lattice constant is 6.47 Å, which is close to the experimental value of 6.44 Å.[23]

## III. RESULTS AND DISCUSSION

The metallic states are reproduced by our band structure calculation for $Pt_{0.99}Ir_{0.01}Sb_2$, see Fig. 1, while undoped

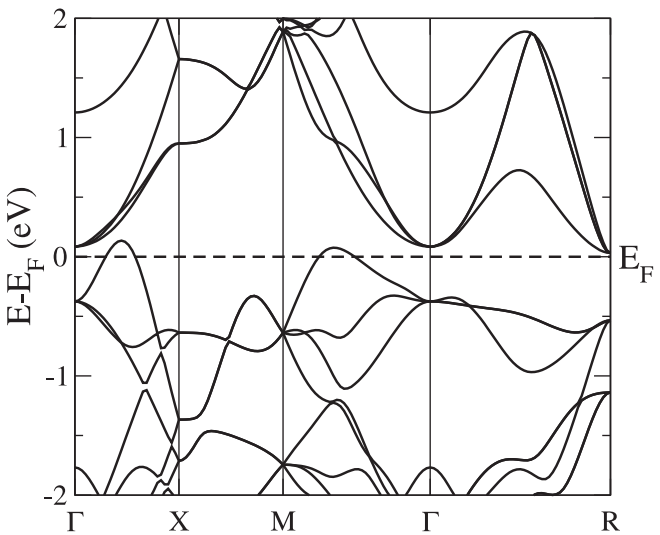


FIG. 1. Band structure of doped $Pt_{0.99}Ir_{0.01}Sb_2$.

a)udo.schwingenschlogl@kaust.edu.sa. Tel.: +966(0)544700080.

 

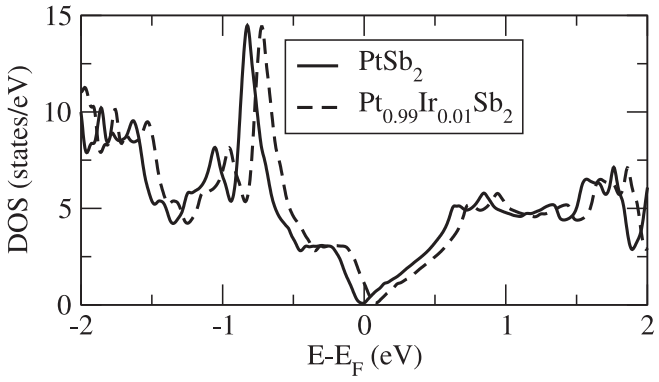


FIG. 2. Density of states of undoped and doped $PtSb_2$.

$PtSb_2$ is an insulator with an experimental band gap of 110 meV at $T \approx 10$ K.[24] Already a small doping of 0.04 holes per unit cell results in a metallic state.[3] Similarly, a small *n*-doping also results in a metallic state.[10] The bands near the Fermi energy ($E_F$) mainly are due to the Sb 5*p* orbitals, with some admixtures of the Pt 5*d* orbitals. The band that crosses $E_F$ originates completely from the Sb 5*p* orbitals throughout the symmetry lines Γ-X-M-Γ. Mori and coworkers have shown that the bands at $E_F$ are corrugated and not the pudding mold type bands that establish the high Seebeck coefficients in $Na_xCoO_2$ (Ref. 2) and $K_xRhO_2$.[25,26] Calculated densities of states (DOSs) of $PtSb_2$ and $Pt_{0.99}Ir_{0.01}Sb_2$ are shown in Fig. 2. It is clearly visible that doping does not change the shape of the DOS but only the position of $E_F$, justifying our usage of the rigid band approximation.

The calculated Seebeck coefficient of $PtSb_2$ in a doping range from 0.04 to 0.4 electrons/holes per unit cell for a temperature range from 300 to 800 K is plotted in Figs. 3(a) and 4(a). Note that a doping of 0.04 electrons/holes per unit cell is equivalent to a carrier concentration of $1.5 \times 10^{20}$ cm$^{-3}$ (as obtained experimentally for $Pt_{0.99}Ir_{0.01}Sb_2$ (Ref. 3)). We find that *S* shows a maximum a bit above 100 $\mu$V/K for each doping level, except for dopings of 0.3 and 0.4 electrons/holes per unit cell, but at different temperatures. This is due to the fact that the conduction band close to $E_F$ gives a negative contribution to the Seebeck coefficient at different temperatures and doping levels.

For $n_h = 0.04$ holes per unit cell, our calculation gives at room temperature a value of $S = 122.5$ $\mu$V/K, which roughly agrees with the experiment (100 $\mu$V/K).[3] Our maximum *S* value is 129.7 $\mu$V/K, while the experimental value is 112 $\mu$V/K at 400 K. For $n_h = 0.04$, the value of *S* remains high up to 450 K and decreases thereafter. Overall, Fig. 3(a) shows that with increasing hole doping the Seebeck coefficient decreases at room temperature, which is also consistent with the experiment. Importantly, the maximal *S* value can be obtained at different temperatures by controlling the carrier concentration, which helps to achieve an optimal performance of the thermoelectric device under different

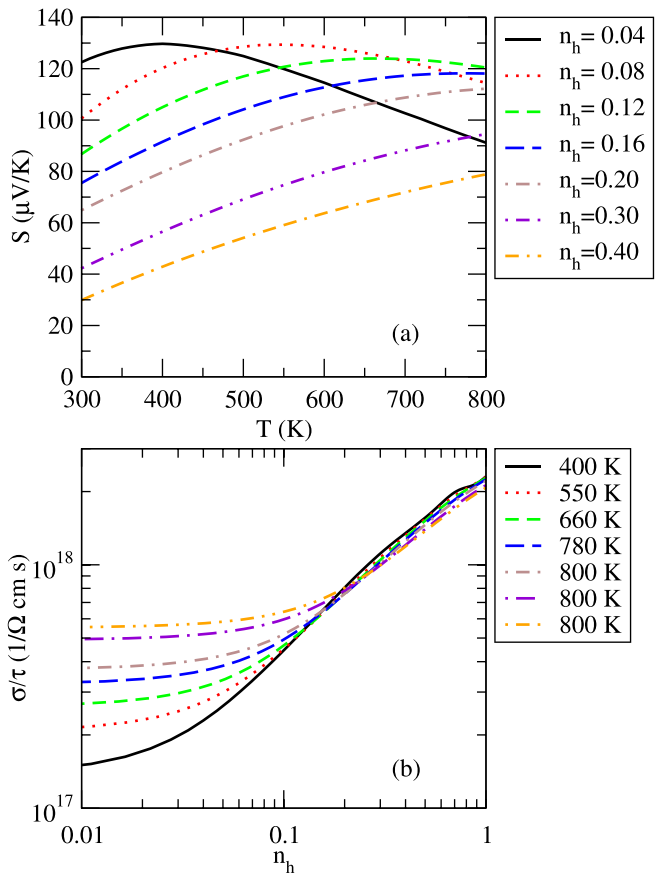


FIG. 3. Calculated *S* and $\sigma/\tau$ of hole doped $PtSb_2$. The number of holes per unit cell is denoted by $n_h$.

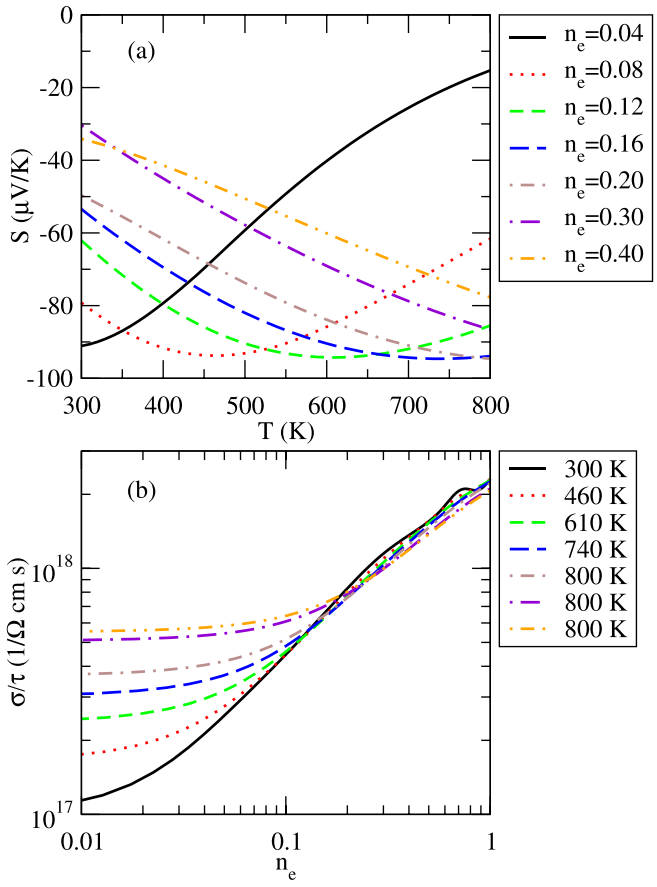


FIG. 4. Calculated *S* and $\sigma/\tau$ of electron doped $PtSb_2$. The number of electrons per unit cell is denoted by $n_e$.

conditions. In Fig. 3(b), we examine the effect of hole doping on the electrical conductivity $\sigma/\tau$ at the temperatures for which we have obtained the highest $S$ for each doping. We find variations with the temperature in the case of low doping, with the highest value at 800 K. For $n_h \gtrsim 0.2$, the value of $\sigma/\tau$ increases rapidly and becomes virtually identical for the considered temperatures. We note also the unusual temperature dependence (significant increase) of $\sigma/\tau$ at low doping. This is due to bipolar conduction, which increases substantially at higher temperatures. The high temperature $ZT$ predictions are generally in a doping range sufficiently heavy to preclude bipolar conduction, as this is destructive to the thermoelectric performance.

As it is experimentally known that both types of doping are possible in $PtSb_2$, we also consider electron doping, which has not been addressed experimentally. Nishikubo and coworkers have shown that the substitution of Sn at the Sb site results in a small powerfactor.[3] This suggests that substitution at the Pt site is more favorable for the transport properties. Hence, we study the substitution of Au at the Pt site, see Figs. 4(a) and 4(b). At room temperature, we find for $n_e = 0.04$, 0.12, and 0.4, values of $S = -91\ \mu$V/K, $-62\ \mu$V/K, and $-34\ \mu$V/K, respectively. This decreasing trend of $S$ with increasing doping is similar to our observations for hole doping. The maximal $S$ is always found around $-94\ \mu$V/K, except for $n_e = 0.3$ and 0.4, in the considered temperature range. It shifts more and more to higher temperature with increasing doping. The variation of $\sigma/\tau$ with the electron concentration and temperature is similar to the case of hole doping.

It is fruitful to compare electron and hole doping in $PtSb_2$ for possible applications in thermoelectric generators with the same host material. In Figs. 5(a)–5(d), we present $S^2\sigma$ and $ZT$ of doped $PtSb_2$ in a doping range from 0.04 to 0.4 electrons/holes per unit cell and temperature range from 300 K to 800 K. For a realistic description of the conductivity, we vary the mobility with respect to the carrier concentration and temperature. Whereas the electronic contribution $\kappa_{el}$ is deduced from the Wiedemann-Franz relation, the phononic contribution is taken from the experiment and varied as $\kappa_{ph} \propto T^{-1}$. Details of the methodology can be found in Ref. 27. According to Fig. 5(a), the calculated room temperature $S^2\sigma$ for $n_h = 0.40$ is $31\ \mu$W/cmK$^2$, which is in excellent agreement with the experimental value of $35\ \mu$W/cmK$^2$. For all other doping levels, $S^2\sigma$ decreases with temperature, as in the experiment. In the case of electron doped $PtSb_2$, the value of $S^2\sigma$ reaches up to $17\ \mu$W/cmK$^2$ for low doping, which is about half the value obtained for hole doping, while at higher doping the electron and hole doped materials exhibit a $S^2\sigma$ of similar magnitude at room temperature. Importantly, $S^2\sigma$ shows the opposite temperature trend for a doping of 0.04 (both electron and hole) as compared to the other doping levels. The room temperature $ZT$ for a doping of 0.04 holes per unit cell is about 0.1, which is in good agreement with the experimental value of 0.12. For doping levels between 0.12 and 0.2 electrons/holes per unit cell, a large $S^2\sigma$ at 800 K results

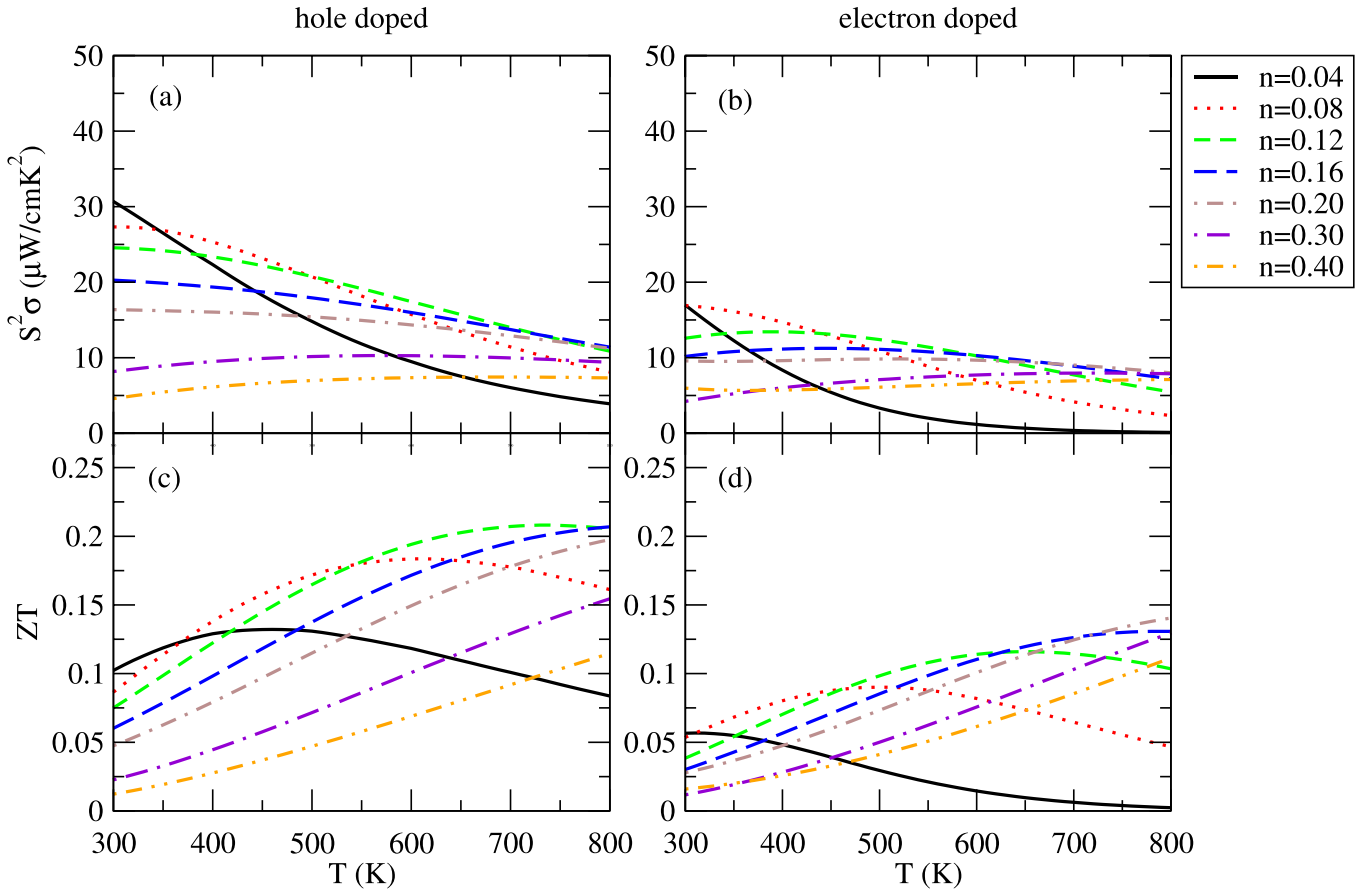


FIG. 5. Calculated $S^2\sigma$ and $ZT$ for electron and hole doped $PtSb_2$ as functions of the temperature for several doping levels.

in a high *ZT* of 0.1/0.2, which is more than twice the room temperature value. A further enhancement of *ZT* by reduction of the thermal conductivity may be achieved in nanostructured $PtSb_2$.

The previous discussion demonstrates a relatively low performance of $PtSb_2$, primarily due to two factors: its comparatively large 300 K lattice thermal conductivity of approximately 7.5 W/mK and the lack of a band gap, which severely limits the Seebeck coefficient. Experimentally, $PtSb_2$ appears to have a small band gap of ~0.1 eV, which we are unable to reproduce. However, in practice, the large lattice thermal conductivity will strongly hamper performance at all but the highest temperatures, where the slight calculational discrepancy will have little effect. There is, however, an opportunity for significant *ZT* enhancement via alloying with As. $PtAs_2$ is isoelectronic and isostructural to $PtSb_2$, with a somewhat smaller lattice parameter of 5.97 Å. More importantly, however, $PtAs_2$ exhibits a significant band of approximately 0.5 eV (our calculations with the modified Becke-Johnson potential find a band gap of 0.38 eV). This means that the Seebeck coefficients in $PtAs_2$ will not be nearly as impacted by bipolar conduction as in $PtSb_2$, where this effect precludes Seebeck coefficients much higher than 100 $\mu$V/K above room temperature. Given this larger band gap, it is likely that an alloy $PtAs_{2-x}Sb_x$ will have a significant band gap, although the exact value is unknown (and *x*-dependent) and must await experimental investigation. Such alloying would also have a beneficial effect on the lattice thermal conductivity, although the effect is largest at low temperature, while the best performance of $PtAs_{2-x}Sb_x$ is expected at high temperature.

With these effects in mind, we depict in Figs. 6(a) and 6(b) the calculated thermopower of $PtAs_2$ within the constant relaxation time approximation (note that no internal coordinate or lattice parameter optimization was performed) for hole and electron concentrations comparable to those presented for $PtSb_2$. For low temperature (200 to 300 K), the values are comparable to those obtained for the corresponding dopings (per unit cell) for $PtSb_2$. At higher temperature, however, the values continue to rise due to the band gap, exceeding absolute values of 200 $\mu$V/K around 1000 K, for both hole and electron doping. This is a typical value for a high performance thermoelectric, although it is not clear whether appropriate optimization techniques in this family of materials can lead to high performance thermoelectrics (typically described by *ZT* of unity or greater).

Since we are concerned with As alloying, we have included in the figures thermopower results in which the band gap is taken as 0.2 eV, or half of the calculated band gap of $PtAs_2$, as a rough estimate of the band gap of PtAsSb. The p-type thermopower (left panel) still shows values exceeding 200 $\mu$V/K at temperatures of 800 to 1200 K, whereas the corresponding thermopowers for *n*-doping do not exceed 160 $\mu$V/K. It, thus, is likely that for the alloying scenario considered here the *p*-type performance will significantly outstrip the *n*-type performance. A second conclusion to be drawn is that for *n*-doping higher As concentrations (with likely larger band gaps) are more probably optimal than for *p*-doping. We also point out that the likely dominance of the lattice thermal conductivity in the heat transport means that nanostructuring techniques to reduce this term can be helpful. Lastly, as a practical matter, we note the high vapor pressure of the toxic As in the high temperature range, so that great care in sample preparation and measurement is a necessity.

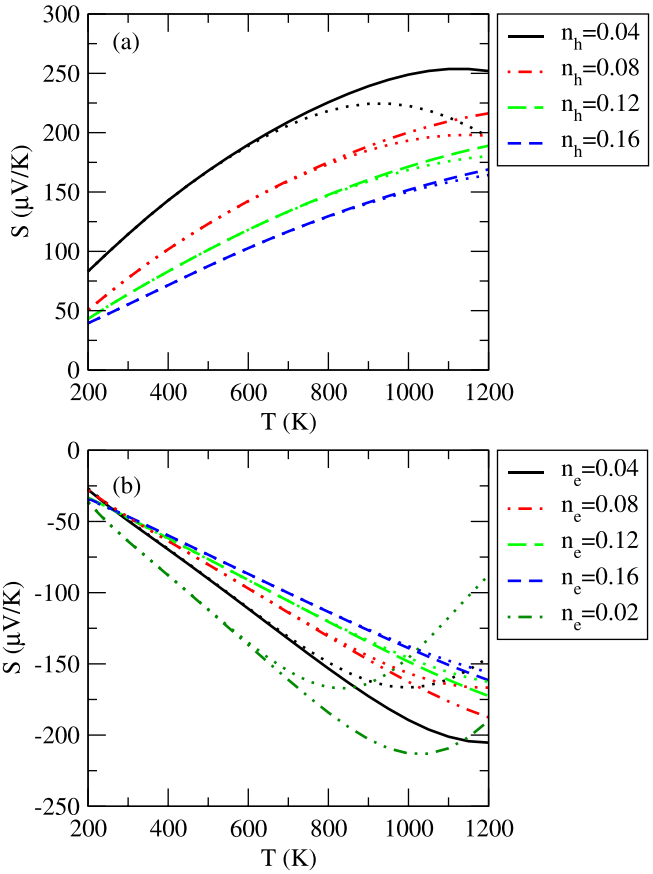


FIG. 6. Calculated thermopower of $PtAs_2$ for several hole and electron doping levels (measured per $PtAs_2$ unit cell). The dotted lines represent results for the electronic structure altered via a scissors shift so that the band gap is 0.2 eV, a rough estimate of the band gap of PtAsSb.

## IV. CONCLUSION

To conclude, we have studied the transport properties of electron and hole doped $PtSb_2$ over a wide doping range. A doping of 0.04 electrons/holes per unit cell gives a high powerfactor at room temperature, which decreases with increasing temperature. Our results show that for doping between 0.12 and 0.2 electrons/holes per unit cell, the *ZT* values, while low, are more than double than those achieved at 800 K, due to a high electrical conductivity. Experiments should be performed at this doping level and temperature range for confirmation. Moreover, it will be desirable to study in more detail nanostructuring strategies in doped $PtSb_2$ to further reduce the thermal conductivity. Finally, we have explored the effect of As alloying, finding that this approach may significantly enhance the performance due to a likely larger band gap.

## ACKNOWLEDGMENTS

This research was supported by the Solid State Solar-Thermal Energy Conversion Center (S3 TEC), an Energy

Frontier Research Center funded by the US Department of Energy, Office of Science, Office of Basic Energy Sciences under Award No. DE-SC0001299/DE-FG02-09ER46577 (DP). Computational resources have been provided by KAUST IT.

[1]K. Nouneha, A. H. Reshak, S. Auluck, I. V. Kityk, R. Viennois, S. Benet, and S. Charar, J. Alloys Compd. **437**, 39 (2007).
[2]K. Kuroki and R. Arita, J. Phys. Soc. Jpn. **76**, 083707 (2007).
[3]Y. Nishikubo, S. Nakano, K. Kudo, and M. Nohara, Appl. Phys. Lett. **100**, 252104 (2012).
[4]D. H. Damon, R. C. Miller, and P. R. Emtage, Phys. Rev. B **5**, 2175 (1972).
[5]C. T. Elliott and S. E. R. Hiscocks, J. Mater. Sci. **3**, 174 (1968).
[6]A. A. Abdullaev, L. A. Angelova, V. K. Kuznetsov, A. B. Ormont, and Y. I. Pashintsev, Phys. Status Solidi A **21**, 339 (1974).
[7]A. Dargys and J. Kundrotas, J. Phys. Chem. Solids **44**, 261 (1983).
[8]R. A. Laudise, W. A. Sunder, R. L. Barns, G. W. Kammlott, A. F. Witt, and D. J. Carlson, J. Cryst. Growth **102**, 21 (1990).
[9]P. M. Nikolic, S. S. Vujatovic, D. M. Todorovic, M. B. Miletic, A. Golubovic, A. I. Bojicic, F. Kermendi, S. Duric, K. T. Radulovic, and J. Elazar, Jpn. J. Appl. Phys., Part 1 **36**, 1006 (1997).
[10]M. Søndergaard, M. Christensen, L. Bjerg, K. A. Borup, P. Sun, F. Steglich, and B. B. Iversen, Dalton Trans. **41**, 1278 (2012).
[11]G. A. Slack, in *CRC Handbook of Thermoelectrics*, edited by D. M. Rowe (CRC Press, Boca Raton, 1995), p. 407.
[12]D. H. Damon, R. C. Miller, and A. Sagar, Phys. Rev. **138**, A636 (1965).
[13]P. Blaha, K. Schwarz, G. Madsen, D. Kvasicka, and J. Luitz, *WIEN2K, An Augmented Plane Wave + Local Orbitals Program for Calculating Crystal Properties* (TU Vienna, Vienna, 2001).
[14]J. P. Perdew, K. Burke, and M. Ernzerhof, Phys. Rev. Lett. **77**, 3865 (1996).
[15]N. J. Ramer and A. M. Rappe, Phys. Rev. B **62**, R743 (2000), and references therein.
[16]L. Chaput, P. Pécheur, J. Tobola, and H. Scherrer, Phys. Rev. B **72**, 085126 (2005).
[17]L. Jodin, J. Tobola, P. Pécheur, H. Scherrer, and S. Kaprzyk, Phys. Rev. B **70**, 184207 (2004).
[18]G. K. H. Madsen and D. J. Singh, Comput. Phys. Commun. **175**, 67 (2006).
[19]G. K. H. Madsen, K. Schwarz, P. Blaha, and D. J. Singh, Phys. Rev. B **68**, 125212 (2003).
[20]T. J. Scheidemantel, C. Ambrosch-Draxl, T. Thonhauser, J. V. Badding, and J. O. Sofo, Phys. Rev. B **68**, 125210 (2003).
[21]D. J. Singh, Phys. Rev. B **76**, 085110 (2007).
[22]L. Zhang, M.-H. Du, and D. J. Singh, Phys. Rev. B **81**, 075117 (2010).
[23]N. E. Brese and H. G. von Schnering, Z. Anorg. Allg. Chem. **620**, 393 (1994).
[24]R. A. Reynolds, M. J. Brau, and R. A. Chapman, J. Phys. Chem. Solids **29**, 755 (1968).
[25]K. Mori, H. Usui, H. Sakakibara, and K. Kuroki, AIP Adv. **2**, 042108 (2012).
[26]Y. Saeed, N. Singh, and U. Schwingenschlögl, Adv. Funct. Mater. **22**, 2792 (2012).
[27]D. Parker and D. J. Singh, Phys. Rev. B **82**, 035204 (2010).